Investigation of the Electronic Structure of PB and AsB using High Resolution Photoelectron Imaging of Cold PB^- and AsB^- Anions

Han-Wen Gao, Jie Hui, Xin-Yu Zhang, and Lai-Sheng Wang[a)]

Department of Chemistry, Brown University, Providence, Rhode Island 02912, USA

[a)] Email: lai-sheng_wang@brown.edu

Abstract

We report a study on the electronic structure and chemical bonding of the PB and AsB diatomic molecules using high-resolution photoelectron imaging of cryogenically-cooled PB^- and AsB^- anions. The electron affinities of PB and AsB are measured to be 2.751(1) and 2.600(1) eV, respectively. The ground states of the PB^- and AsB^- anions are determined to be $^2\Sigma^+$ with a $\sigma^1\pi^4$ valence electron configuration. The ground states of neutral PB and AsB are found to be $^3\Pi_2$ with a $\sigma^1\pi^3$ electron configuration. The spin-orbit excited states ($^3\Pi_1$ and $^3\Pi_0$), as well as two low-lying singlet excited states ($^1\Sigma^+$ and $^1\Pi$) are observed. Unusual spectroscopic characteristics are observed in the $^3\Pi_2$ ground state of AsB, probably due to state mixing with a higher-lying $^1\Delta_2$ state. The current work provides extensive electronic and spectroscopic information for the PB and AsB molecules.

I. INTRODUCTION

The group III-V compounds are important semiconductor materials. As their fundamental building blocks, group III-V diatomic molecules have been extensively investigated.[1-10] Anion photoelectron spectroscopy (PES) is a powerful technique to probe the electronic structure of matter and has been used to study the AlP^-, GaP^-, InP^-, and $GaAs^-$ anions,[5] as well as the heavy isovalent $SnPb^-$ anion.[6] In these diatomic species, chemical bonding primarily arises from the valence *p* orbitals and spin-orbit coupling was found to play an important role. Borides of group V elements have recently garnered increased attention because cubic boron arsenide has been discovered to exhibit ultrahigh thermal conductivity and high ambipolar mobility.[11-13] Among all group V boride diatomic species, NB has received the most extensive experimental[7,8] and theoretical attention.[14] The NB^- anion has been investigated by PES,[7] revealing that the diatomic anion has a $^2\Sigma^+$ ground state with a $\sigma^1\pi^4$ valence electron configuration. The neutral NB molecule was found to have a $^3\Pi$ ground state, with its first excited state ($^1\Sigma^+$) lying closely to the ground state. We have recently studied the heavy BiB^- species using high-resolution photoelectron imaging[9] and found that the ground state of BiB^- is $^2\Pi$ with a $\sigma^2\pi^3$ valence electron configuration, different from that of the lighter NB^-. Due to the open-shell nature and strong spin-orbit coupling, the PES of BiB^- was much more complicated in comparison to that of NB^-. We identified the ground state [$^3\Sigma^-(0^+)$] of BiB, along with eight low-lying excited states [$^3\Sigma^-(1)$, $^3\Pi(2)$, $^3\Pi(1)$, $^3\Pi(0^-)$, $^3\Pi(0^+)$, $^1\Delta(2)$, $^1\Sigma^+(0)$,$^1\Pi(1)$] due to spin-orbit and spin-spin coupling. The change of the valence electron configuration from $\sigma^1\pi^4$ in NB^- to $\sigma^2\pi^3$ in BiB^- reflects the relative stability of the valence σ and π orbitals going down the periodic table and carries important information about the chemical bonding in the III-V diatomic species. The NB and BiB diatomics represent the interactions of boron with the lightest and heaviest group V elements, respectively. However, relatively little is known about the intermediate B-V diatomic species. The only prior experimental investigation was on PB using the Knudsen-cell mass spectrometric technique, which determined its dissociation energy and provided an upper limit for its ionization energy,[10] although there have been several theoretical calculations on PB and AsB.[15-17]

In the current article, we report the first PES study on PB^- and AsB^-, using high-resolution photoelectron imaging (PEI) of cryogenically-cooled anions. Previous PES studies on the III-V diatomics faced challenges in spectral assignments due to vibrational hot bands and spin-orbit splitting, making it difficult to distinguish electronic states from vibrational features. By coupling a cryogenically-cooled 3D Paul trap with a laser vaporization cluster source,[9,18] we can prepare vibrationally-cold anions, enabling high spectral resolution and definitive assignments. We find the ground state of PB^- and AsB^- to be $^2\Sigma^+$ with a $\sigma^1\pi^4$ valence electron configuration and that of neutral PB and AsB to be $^3\Pi_2$ with a $\sigma^1\pi^3$ electron configuration. The electron affinities of PB and AsB are measured to be 2.751(1) and 2.600(1) eV, respectively. Four electronic excited states are also observed ($^3\Pi_1$, $^3\Pi_0$, $^1\Sigma^+$, and $^1\Pi$) for both PB and AsB, as well as their vibrational frequencies. The vibrationally-resolved PEI allows us to probe the nature of the valence σ and π orbitals in the intermediate B-V diatomic molecules.

II. EXPERIMENTAL METHOD

High-resolution PES experiments were performed using a PEI apparatus newly equipped with a cryogenically-cooled 3D Paul trap. The PEI apparatus has been reported in detail previously.[19] The recent addition of a cryogenically-cooled 3D Paul trap has been shown to be critical to prepare vibrationally-cold anionic clusters produced from a laser vaporization source, in particular for diatomic species and small clusters.[9,18] In this study, we generated the PB^- and AsB^- anions by laser vaporization of disk targets made by mixing powders of phosphorus or arsenic with isotope-enriched boron. Phosphorus was mixed with ^{10}B-enrich boron and arsenic was mixed with ^{11}B-enriched boron to avoid potential mass degeneracy from impurities. Helium carrier gas was used to quench the laser-induced plasma to initiate cluster formation. Clusters formed inside the nozzle were entrained by the carrier gas and underwent a supersonic expansion. After passing through a skimmer, the collimated cluster beam traveled directly into a 3D Paul trap cooled down to 4.2 K by a two-stage closed-cycle helium refrigerator. The trapped anions were collisionally cooled by a mixed He/H_2 buffer gas (4:1 by volume) for 45 ms before being pulsed into the extraction region of a time-of-flight mass spectrometer. The PB^- and AsB^- anions were mass-selected and intercepted by a detachment laser in the interaction zone of a velocity-map imaging (VMI) system. Photodetachment was performed using a YAG-pumped dye laser, as well as the third harmonic output from a Nd:YAG laser. Photoelectrons were projected onto a set of microchannel plates coupled with a phosphor screen and a charge-coupled-device camera. A typical experiment required about 100,000–300,000 laser shots to achieve reasonable signal-to-noise ratios. The VMI lens was calibrated using the PE images of Bi^- at various photon energies. The PE images were analyzed by the maximum entropy method (MEVELER).[20] The resolution of the VMI system was ~0.6 % for electrons with high kinetic energies and as low as 1.2 cm^{-1} for very slow electrons.[19]

Photoelectron angular distributions (PADs) are obtained from the PE images, which are characterized by the anisotropy parameter (β).[21] The differential cross section of the photoelectrons can be expressed as

$$d\sigma/d\Omega = (\sigma_{Tot}/4\pi)[1 + \beta P_2(\cos\theta)] \quad (1)$$

where σ_{Tot} is the total cross section, P_2 is the second-order Legendre polynomial, and θ is the angle of the photoelectron relative to the laser polarization. Thus, the PADs can be described by:

$$I(\theta) \sim [1 + \beta P_2(\cos\theta)] \quad (2)$$

where β has a value ranging from −1 to 2. This model works well for single-photon ionization of randomly oriented molecules. According to the electric dipole selection rules, when an electron in an atom with angular momentum l is detached, the outgoing photoelectron wave must carry an angular momentum of $l \pm 1$. For example, if an electron is detached from an s atomic orbital ($l = 0$), the outgoing photoelectron will have $l = 1$ (pure p-wave) with $\beta = 2$. If an electron is detached from an atomic p orbital, the outgoing electron will carry s+d partial waves with $\beta = -1$. While it is generally non-trivial to interpret the β parameter for electron

detachment from molecular orbitals (MOs),[22] which are linear combinations of atomic orbitals, the PADs are particularly valuable for diatomic species, whose MOs have well-defined angular momenta.

III. RESULTS

A. PEI of PB^-

Figure 1 displays the PE images and spectra of PB^- at two photon energies. In the 3.496 eV spectrum (Fig. 1b), three electronic states (X, C, and D) can be identified on the basis of their angular distributions and relative spacing, each followed by a vibrational progression. Peaks X and *a* exhibit similar (*s*+*d*)-type angular distributions with negative β parameters, with a spacing of 952 cm^{-1}. Thus, peak X should be the 0-0 transition to the ground electronic state of PB and peak *a* is due to vibrational excitation of the neutral PB ground state. The weak peak *a*' at the low binding energy side should be due to a vibrational hot band of PB^-. We estimated a vibrational temperature of ~80 K for the BiO_2^- and SbO_2^- anions even when the ion trap was operated at 4.2 K.[18a,18b] However, without the cryogenic cooling we showed that we could only cool the Au_2^- anion to a vibrational temperature of 175 K in our laser vaporization supersonic cluster source.[23] Peaks C and *b* display similar *p*-type angular distributions with positive β parameters. Thus, peak C should correspond to an excited state of PB and peak *b* defines its vibrational frequency (1049 cm^{-1}). Similarly, peaks D and *c* exhibit similar (*s*+*d*)-type angular distributions with negative β parameters, and they should represent another excited state of PB with a vibrational frequency of 948 cm^{-1}.

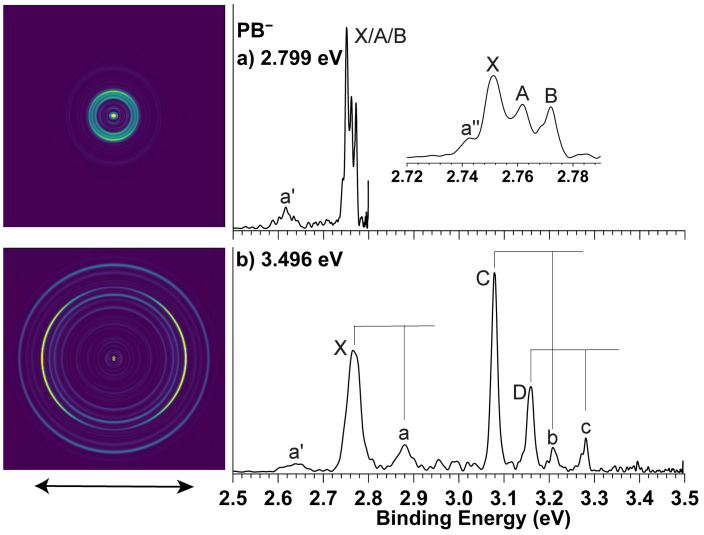

FIG. 1. Photoelectron images and spectra of cryogenically-cooled PB^- at a) 2.799 eV and b) 3.496 eV. The double arrow below the images indicates the laser polarization.

In the 2.799 eV spectrum (Fig. 1a), peak X is resolved into three main components (X, A, B) along with a shoulder (*a*'') on the high binding energy side. The splittings between peak X and A and between A and B are 0.011 eV and 0.010 eV, respectively. Their similar spacings

and similar PADs suggest they likely come from spin-orbit splittings. Peak X in the 2.799 eV spectrum defines an accurate EA of 2.751 eV for PB. Peak *a* should also contain similar spin-orbit splitting components as peaks X, A and B, but they are not resolved in the 3.496 eV spectrum (Fig. 1b). Additionally, the hot band *a′* should be due to the transition from $v' = 1$ of the anion to $v = 0$ of the neutral ground state (1_1^0), whereas the *a″* shoulder should be due to the 1_1^1 transition, indicating that the vibrational frequency of the anion is larger than that of the neutral ground state. The binding energies, vibrational frequencies, β parameters, and the assignment of all the observed spectral features are summarized in Table I.

TABLE I. The measured binding energies (BE) and assignment of the observed PES peaks of PB^-. The energy shift (ΔE) relative to peak X, vibrational frequency of each electronic state and the β value are also given.

Peak	Assignment	BE (eV)[a]	ΔE (eV)	Frequency (cm^{-1})[a]	β[b]
a'	1_1^0	2.617(4)	-0.134	1080(30)[c]	
a″	1_1^1	2.742(2)	-0.009		
X	$^3\Pi_2$	2.751(1)	0		-0.5
A	$^3\Pi_1$	2.762(1)	0.011		-0.5
B	$^3\Pi_0$	2.772(1)	0.021		-0.5
a	$^3\Pi(1_0^1)$	2.880(3)		952(30)[d]	-0.4
C	$^1\Sigma^+$	3.079(1)	0.328		1.7
D	$^1\Pi$	3.159(1)	0.408		-0.4
b	$^1\Sigma^+(1_0^1)$	3.209(1)		1049(8)	0.7
c	$^1\Pi(1_0^1)$	3.281(1)		984(8)	-0.3

[a] The numbers in the parentheses represent the uncertainty in the last digit.
[b] β parameters are obtained from the PE image taken at 3.496 eV.
[c] The vibrational frequency of the $P^{10}B^-$ anion.
[d] Because the spin-orbit components of peak *a* are not resolved, the vibrational frequency is estimated using the averaged binding energy of peaks X, A and B.

B. PEI of AsB^-

Figure 2 displays the PE images and spectra of AsB^- at three photon energies. The 3.204 eV spectrum (Fig. 2c) follows a pattern similar to that of PB^-, featuring three closely-lying states at lower binding energies (X, A, B) and two excited states at higher binding energies (C, D). The splittings among X, A, B are larger than those in the spectra of PB^- (Fig. 1) and their vibrational progressions overlap, resulting in considerable spectral congestion. Peaks C and *d* have similar *p*-type angular distributions, which should correspond to an excited state of AsB with a vibrational frequency of 855 cm^{-1}. Peaks D and *c* have similar (*s*+*d*)-type angular distributions with negative β parameters, and they should come from another excited state of

AsB with a vibrational frequency of 948 cm^{-1}. The weak peaks *a′* and *b′* at lower binding energies should come from vibrational hot bands.

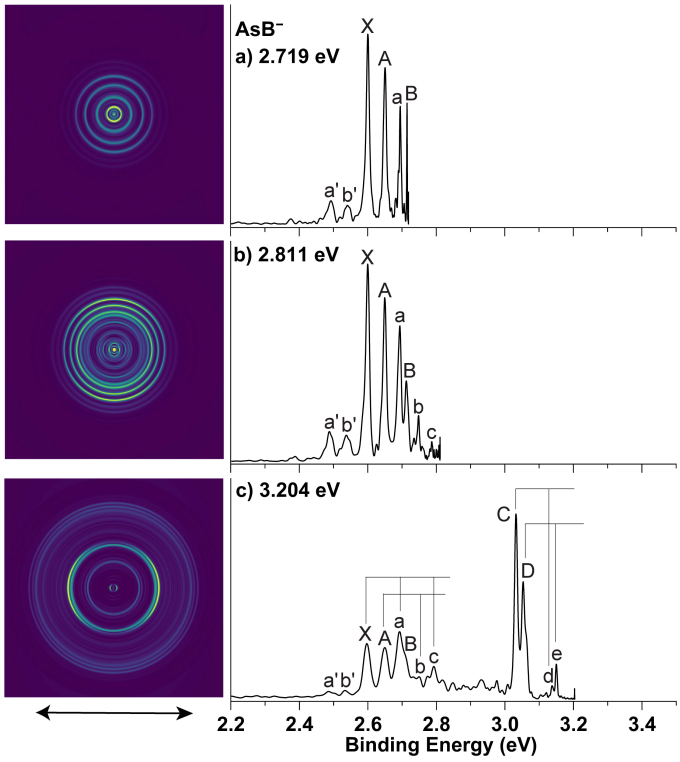

FIG. 2. Photoelectron images and spectra of cryogenically-cooled AsB^- at a) 2.719 eV, b) 2.811 eV and c) 3.204 eV. The double arrow below the images indicates the laser polarization.

The 2.811 eV (Fig. 2b) and 2.719 eV spectra (Fig. 2a) are taken to resolve better the electronic and vibrational features for the X, A, and B states. Peak X represents the 0-0 transition to the ground electronic state of AsB, yielding an EA of 2.600 eV for AsB. Following peak X, a prominent vibrational progression (peaks *a* and *c*) is observed with a vibrational frequency of 754 cm^{-1} for the AsB ground state. The splittings between peaks X and A and between A and B are 0.050 eV and 0.063 eV, respectively, which are larger than those in PB, as expected for spin-orbit splittings. Peak A is accompanied by a vibrational progression (peak *b*), yielding a vibrational frequency of 790 cm^{-1}.

Notably, the vibrational progression for the ground state X (peaks *a* and *c*) are much more prominent. Furthermore, peaks *a* and *c* display isotropic or even *p*-type angular distributions, which differ from those of the nearby peaks. As will be discussed later, the anomalous Frank-Condon factors and angular distributions suggest strong mixing of the AsB ground state with some higher excited states. The binding energies, vibrational frequencies, β parameters, and the assignment of all the observed spectral features are summarized in Table II.

IV. DISCUSSION

A. Assignment of the PES of PB^- and AsB^-

The valence electron configurations of P and As are $3s^23p^3$ and $4s^24p^3$, and that of B is

TABLE II. The measured binding energies (BE) and assignment of the observed PES peaks of AsB^-. The energy shift (ΔE) relative to peak X, vibrational frequency of each electronic state and the β value are also given.

Peak	Assignment	BE (eV)[a]	ΔE (eV)	Frequency (cm^{-1})[a]	β[b]
a'	1_1^0 ($^3\Pi_2$)	2.488(4)	-0.112	900(20)[c]	-0.4
b'	1_1^0 ($^3\Pi_1$)	2.538(4)	-0.062		-0.1
X	$^3\Pi_2$	2.600(1)	0		-0.5
A	$^3\Pi_1$	2.650(1)	0.050		-0.5
a	$^3\Pi_2(1_0^1)$	2.694(1)		754(8)[d]	0.1
B	$^3\Pi_0$	2.713(1)	0.113		-0.4
b	$^3\Pi_1(1_0^1)$	2.748(1)		790(8)	-0.5
c	$^3\Pi_2(1_0^2)$	2.787(1)			0.3
C	$^1\Sigma^+$	3.032(1)	0.432		1.3
D	$^1\Pi$	3.053(1)	0.453		0.0
d	$^1\Sigma^+(1_0^1)$	3.138(1)		855(8)	0.8
e	$^1\Pi(1_0^1)$	3.150(1)		782(8)	0.1

[a] The numbers in the parentheses represent the uncertainty in the last digit.
[b] β parameters are obtained from the PE image taken at 3.204 eV, except for peak B and peak *b*, which cannot be resolved clearly in the 3.204 eV spectrum. β parameters for peak B and peak *b* are determined from the PE image taken at 2.811 eV
[c] The vibrational frequency of the $As^{11}B^-$ anion.
[d] This frequency is the average value determined by peak *a* and peak *c*.

$2s^22p^1$. In the MB (M = P, As) diatomic molecules, the valence *n*s and 2s orbitals combine to form a σ bonding and a σ* antibonding orbital, both of which are fully occupied, whereas the 2p and *n*p orbitals form one σ and two π bonding orbitals, along with the σ* and π* antibonding orbitals. The five p electrons in the MB^- anions fill the bonding σ and π orbitals to give either a $\sigma^1\pi^4$ or $\sigma^2\pi^3$ valence electron configuration, resulting in the following one-electron detachment channels to the neutral final states:

$$\sigma^2\pi^3\ (^2\Pi) \rightarrow \sigma^2\pi^2\ (^3\Sigma^-, {}^1\Delta, {}^1\Sigma^+) \quad (3)$$

$$\rightarrow \sigma^1\pi^3\ (^3\Pi_{0,1,2}, {}^1\Pi) \quad (4)$$

$$\sigma^1\pi^4\ (^2\Sigma^+) \rightarrow \sigma^1\pi^3\ (^3\Pi_{0,1,2}, {}^1\Pi) \quad (5)$$

$$\rightarrow \sigma^0\pi^4\ (^1\Sigma^+) \quad (6)$$

The previous PES studies on the isovalent III-V heavy diatomic species indicate that transitions from the anion ground state to triplet neutral states occur at lower binding energies than those to singlet states.[5,6,9] Both the PB^- and AsB^- PE spectra show three closely-lying

states at lower binding energies, followed by two additional states at higher binding energies. The similar PES patterns observed for PB^- and AsB^- suggest they have similar electronic structures. In fact, our observed spectral patterns are consistent with the detachment channels from the $\sigma^1\pi^4$ ($^2\Sigma^+$) configuration of the anion, which produces a triplet $^3\Pi$ neutral ground state and two singlet excited states ($^1\Pi$ and $^1\Sigma^+$). Spin-orbit coupling will split the triplet $^3\Pi$ final state into three $^3\Pi_0$, $^3\Pi_1$ and $^3\Pi_2$ components. In contrast, detachment from the $\sigma^2\pi^3$ ($^2\Pi$) configuration of the anion would result in a greater number of final states than those observed experimentally.

Therefore, using the $\sigma^1\pi^4$ anion electron configuration, we can assign the observed PES features of PB^- and AsB^- straightforwardly. Detachment of an electron from the π orbital results in the $^3\Pi_{0,1,2}$ states (eq. 5), consistent with the (*s*+*d*) angular distributions observed for peaks X, A, and B in the PES of both PB^- and AsB^-. According to Hund's rules, the $^3\Pi_2$ spin-orbit state should be the ground state. Thus, peaks X, A, and B should correspond to $^3\Pi_2$, $^3\Pi_1$, and $^3\Pi_0$, respectively. Detachment from the π orbital can also result in the $^1\Pi$ state (eq. 5) with the same (*s*+*d*) angular distributions as the $^3\Pi$ state, i.e. peak D. Thus, peak C should be due to detachment from the σ orbital, resulting in the $^1\Sigma^+$ final state (eq. 6), as evidenced by the *p*-type angular distribution. The spectral assignments for all the observed PES features are given in Table I and Table II for PB and AsB, respectively. In general, the energy spacing between the spin-orbit states should be constant, as revealed by the separations among the $^3\Pi_{2,1,0}$ spin-orbit states in PB (Table I). However, the spacing between the $^3\Pi_2$ and $^3\Pi_1$ states (0.050 eV) in AsB is notably smaller than that between the $^3\Pi_1$ and $^3\Pi_0$ states (0.063 eV) (Table II). This difference is likely due to an off-diagonal spin-orbit interaction between the $^3\Pi_1$ state and the high-lying $^1\Pi_1$ state originated from the same electronic configuration ($\sigma^1\pi^3$), which can stabilize the $^3\Pi_1$ state.[24]

Figure 3 summarizes all the detachment transitions from the ground state of PB^- and AsB^- to the ground and low-lying electronic states of their corresponding neutrals observed in the current study. Table III summarizes all the spectroscopic information for PB and AsB obtained in the current study, in comparison with previous theoretical results where available. A number of theoretical calculations have been performed on PB, with the most comprehensive study being conducted at the MRCI+Q/aV6Z level of theory.[16] While fewer calculations on AsB have been reported, there has been a study at the MRCI+Q/cc-pV5Z level.[17] The calculated excitation energies of the low lying states of BP and AsB and other spectroscopic constants are compared with the current experimental results in Table III. Due to the nearly degenerate molecular orbitals and closely spaced electronic states, these molecules are expected to exhibit strong multi-reference characteristics. Overall, the MRCI calculations show good agreement with the experimental results, highlighting the importance of multi-reference methods in accurately describing the electronic structures of PB and AsB.

B. The chemical bonding in PB^- and AsB^-

The vibrational information obtained in the current study provides valuable insight into the chemical bonding between B and P or As. The PB^- anion has a valence electronic

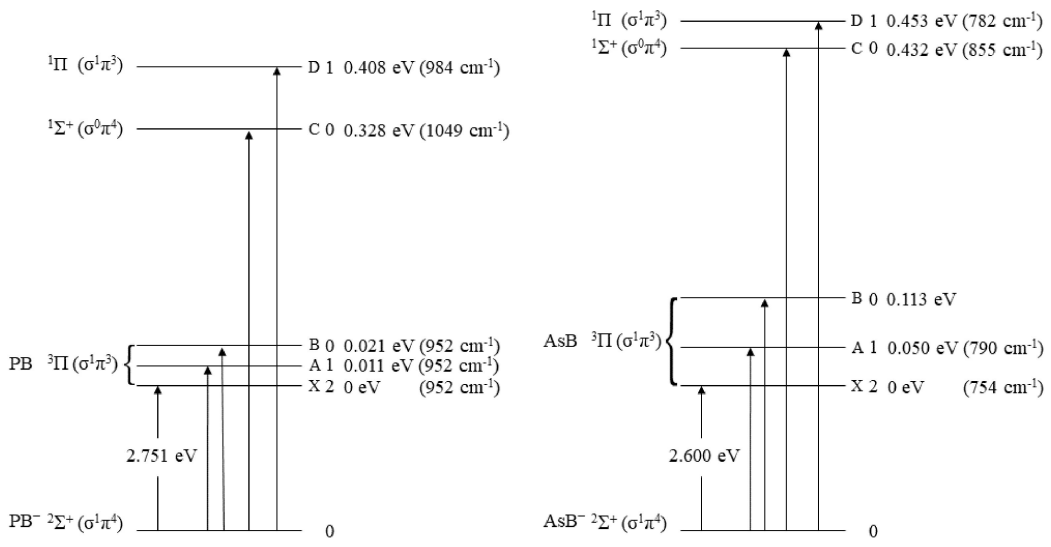

Fig. 3. Schematic energy level diagrams for the observed detachment transitions from the ground state of PB^- and AsB^- to the low-lying states of PB and AsB. The electronic configurations and electronic states of the anion and the neutral final states, as well as the EAs are given on the left. The observed PES features, the total angular momentum due to spin-orbit coupling, the measured excitation energies of the neutral states and vibrational frequencies are given on the right. Note that the vibrational frequencies are for $P^{10}B$ and $As^{11}B$.

configuration of $\sigma^1\pi^4$, where both the σ and π orbitals are bonding orbitals formed by the valence *p* orbitals of P and B. Detaching an electron from the π orbital yields the $^3\Pi$ and $^1\Pi$ states, each exhibiting a vibrational progression indicative of a bond length change. As shown in Table III, the bond lengths of PB in the $^3\Pi$ and $^1\Pi$ neutral states are 1.75 Å and 1.76 Å, respectively, which are both longer than that of the anion (1.71 Å). The measured vibrational frequency for the neutral ground state (952 cm^{-1}) is also lower than that of the anion (1080 cm^{-1}). These results suggest that the π orbital is a strong bonding orbital, and the detachment of a π electron weakens the P–B bond in neutral PB ground state.

Compared with the π orbital, the nature of the σ orbital is more intriguing. In the PB^- anion, the σ orbital is singly occupied while the π orbital is fully occupied, suggesting that the σ orbital is less stable than the π orbital in this configuration ($\sigma^1\pi^4$). However, the transition to the neutral ground state, with a configuration of $\sigma^1\pi^3$, occurs via electron removal from the π orbital, indicating that the σ orbital is more stable than the π orbital in this configuration ($\sigma^1\pi^3$). This observation suggests that in the MO diagram, the σ and π orbitals are close in energy, with their relative stability depending on electron occupancy.[14c] Inversions between the σ and π orbitals arise from interactions between the valence *p*-derived σ orbital with the valence *s*-derived lower σ* orbital, which can significantly destabilize the σ orbital while stabilizing the σ* orbital.[25]

In our recent study on BiB^-,[9] which is valence-isoelectronic with PB^-, no vibrational progression was observed upon electron detachment from the σ orbital, suggesting that the σ orbital in BiB^- is nonbonding. Compared with the 3*s* orbital of P, the 6*s* orbital of Bi is highly contracted and stabilized due to the strong relativistic effects,[26] reducing their ability to form strong σ interactions with the 2*s* orbitals of B. Consequently, the σ* orbital is much lower in

TABLE III. The excitation energies and vibrational frequencies of low lying states of BP and AsB, in comparison with those from the theoretical calculations. The calculated bond lengths are also shown.

	PB [a]		AsB [b]	
	Current work[c]	Calculations[d]	Current work[c]	Calculations[e]
EA (eV)	2.751(1)	2.74	2.600(1)	
$^3\Pi_2$ (eV)	0		0	
ω_e (cm^{-1})	952(30)	941	754(8)	777
r_e (Å)		1.75		1.87
$^3\Pi_1$ (eV)	0.011(1)		0.050(1)	
ω_e (cm^{-1})	952(30)	941	790(8)	777
r_e (Å)		1.75		1.87
$^3\Pi_0$ (eV)	0.021(1)		0.113(1)	
ω_e (cm^{-1})	952(30)	941		777
r_e (Å)		1.75		1.87
$^1\Sigma^+$ (eV)	0.328(1)	0.32	0.432(1)	0.33
ω_e (cm^{-1})	1049(8)	1040	855(8)	870
r_e (Å)		1.68		1.79
$^1\Pi$ (eV)	0.408(1)	0.39	0.453(1)	0.36
ω_e (cm^{-1})	984(8)	934	782(8)	777
r_e (Å)		1.76		1.88

[a] The vibrational frequency of the $P^{10}B^-$ anion ground state ($^2\Sigma^+$) is measured to be 1080±30 cm^{-1} (Table 1). The calculated frequency and bond length for the anion ($^2\Sigma^+$) are 1018 cm^{-1} and 1.71 Å from ref. 16. All measured vibrational frequencies are for the ^{10}B isotope, $P^{10}B$.

[b] The vibrational frequency of the $As^{11}B^-$ anion ground state ($^2\Sigma^+$) is measured to be 900±20 cm^{-1} (Table 2). All measured vibrational frequencies are for the ^{11}B isotope, $As^{11}B$.

[c] The numbers in the parentheses represent the uncertainty in the last digit.

[d] From ref. 16. Spin-orbit coupling in the $^3\Pi$ state was not considered in the calculation.

[e] From ref. 17.

energy and has a weaker destabilizing effect on the σ bonding orbital. Thus, the σ orbital in PB should be more destabilized due to stronger σ–σ∗ interactions. In fact, we find that the σ orbital is even somewhat antibonding. In the PES of PB^-, a more pronounced vibrational progression is observed upon detaching an electron from the σ orbital (peak *b* in Figure 1), indicating a bond length change upon electron detachment. While the observed vibrational frequency for the final state (1049 cm^{-1}) is comparable to that of the anion (1080 cm^{-1}), the computed bond length of PB in the $^1\Sigma^+$ state (1.68 Å) is indeed shorter than that of the anion (1.71 Å).[16]

In the PES of AsB^-, the vibrational progression of the $^1\Sigma^+$ state is weaker than that of PB^-, as evidenced by the lower intensity of peak *d* in Figure 2 compared to peak *b* in Figure 1. This suggests that the σ orbital in AsB^- is less antibonding compared to that in PB^-, i.e., between

PB^- and BiB^-. The measured vibrational frequency of the $^1\Sigma^+$ state (855 cm^{-1}) is comparable to that of the AsB^- anion (900 cm^{-1}) (Table III). There is no computed bond length of the AsB^- anion for comparison, but the computed bond length (1.79 Å) for the $^1\Sigma^+$ state is much shorter than that of the ground state (1.87 Å).[17]

C. The unusual electronic ground state of AsB

In the PES of AsB^-, we observe that the $^3\Pi_2$ state displays a large vibrational progression (peaks X, *a* and *c*), where the $v = 1$ level has an unusually large Franck-Condon factor (Fig. 2), in contrast with the other two spin-orbit states ($^3\Pi_1$ and $^3\Pi_0$). Furthermore, the more isotropic angular distributions of the vibrational levels in the $^3\Pi_2$ state differ from those of the other two spin-orbit states. Finally, the vibrational frequency for the $^3\Pi_2$ state (754 cm^{-1}) is significantly lower than that of the $^3\Pi_1$ state (790 cm^{-1}) (Tables II and III). These observations suggest that the $^3\Pi_2$ ground state has a distinctly different potential energy surface compared to its spin-orbit counterparts. In comparison, the PES of PB^- (Figure 1b) shows that all three spin-orbit states ($^3\Pi_2$, $^3\Pi_1$, and $^3\Pi_0$) have similar spacings, similar Franck-Condon factors, and similar angular distributions, as expected.

Off-diagonal interactions can couple states with the same total angular momentum Ω. In addition to the off-diagonal interaction between the $^3\Pi_1$ and the $^1\Pi_1$ states, that can change the spacing of the three spin-orbit states, the $^3\Pi_2$ state may also interact with a higher state with $\Omega = 2$. It turns out that the $^1\Delta_2$ state, which has an electron configuration of $\sigma^2\pi^2$ is computed to lie much closer in energy (1.39 eV) to the $^3\Pi_2$ state compared to that of PB (2.02 eV).[16,17] The energetic proximity suggests that the $^3\Pi_2$ and $^1\Delta$ states in AsB can have significant mixing, thus altering the potential energy curve for the $^3\Pi_2$ ground state. This strong mixing may explain the unusual Franck-Condon factors and angular distributions observed for the $^3\Pi_2$ state in AsB.

V. CONCLUSION

In conclusion, we have investigated the electronic structure and chemical bonding of PB^- and AsB^- as well as their neutral species using high-resolution photoelectron imaging of cryogenically-cooled anions. The PB^- and AsB^- anions are found to have a $^2\Sigma^+$ ground state with a $\sigma^1\pi^4$ valence electron configuration, whereas their neutral ground state is found to be $^3\Pi_2$ ($\sigma^1\pi^3$). Detachment transitions to the $^3\Pi_{0,1,2}$, $^1\Sigma^+$ and $^1\Pi$ states of PB and AsB neutral molecules, as well as their vibrational frequencies, are observed. The electron affinities of PB and AsB are measured to be 2.751(1) and 2.600(1) eV, respectively. The large vibrational frequency and short bond length of the $^1\Sigma^+$ state ($\sigma^0\pi^4$), which arise from electron detachment from the valence *p*-derived σ orbital, suggest that the σ orbital in both PB^- and AsB^- has antibonding characters due to strong $\sigma-\sigma*$ interactions. The $^3\Pi_2$ ground state of AsB is observed to display very different spectroscopic characteristics relative $^3\Pi_1$ and $^3\Pi_0$ spin-orbit states, as a result of interactions with a higher-lying $^1\Delta$ state.

ACKNOWLEDGMENTS

This work was supported by the National Science Foundation (Grant No. CHE-2053541).

AUTHOR DECLARATIONS

Conflict of Interest

The authors have no conflicts to disclose.

Author Contributions

Han-Wen Gao: Conceptualization (lead); Data curation (lead); Formal analysis (lead); Writing–original draft (lead). **Jie Hui:** Data curation (supporting). **Xin-Yu Zhang:** Data curation (supporting). **Lai-Sheng Wang:** Conceptualization (lead); Formal analysis (supporting); Funding acquisition (lead); Writing–original draft (lead).

REFERENCES

1. G. W. Lemire, G. A. Bishea, S. A. Heidecke, and M. D. Morse, J. Chem. Phys. **92**, 121 (1990).
2. M. Ebben and J. J. ter Meulen, Chem. Phys. Lett. **177**, 229 (1991).
3. S. Li, R. J. Van Zee, and W. Weltner, Jr., J. Phys. Chem. **98**, 2275 (1994).
4. S. Li, R. J. Van Zee, and W. Weltner, Jr., J. Phys. Chem. **97**, 11393 (1993).
5. H. Gómez, T. R. Taylor, Y. Zhao, and D. M. Neumark, J. Chem. Phys. **117**, 8644 (2002).
6. J. Ho, M. L. Polak, and W. C. Lineberger, J. Chem. Phys. **96**, 144 (1992).
7. K. R. Asmis, T. R. Taylor, and D. M. Neumark, Chem. Phys. Lett. **295**, 75 (1998).
8. M. Lorenz, J. Agreiter, A.M. Smith, and V.E. Bondybey, J. Chem. Phys. **104**, 3143 (1996).
9. H. W. Gao, H. W. Choi, J. Hui, W. J. Chen, G. S. Kocheril, and L. S. Wang, J. Chem. Phys. **159**, 114301 (2023).
10. K. A. Gingerich, J. Chem. Phys. **56**, 4239 (1972).
11. L. Lindsay, D. A. Broido, and T. L. Reinecke, Phys. Rev. Lett. **111**, 025901 (2013).
12. F. Tian, et al., Science **361**, 582 (2018).
13. J. Shin, et al., Science **377**, 437 (2022).
14. (a) J. M. L. Martin, T. J. Lee, G. E. Scuseria, and P. R. Taylor, J. Chem. Phys. **97**, 6549 (1992); (b) C. W. Bauschlicher, Jr. and H. Partridge, Chem. Phys. Lett. **257**, 601 (1996); (c) Z. Gan, D. J. Grant, R. J. Harrison, and D. A. Dixon, J. Chem. Phys. **125**, 124311 (2006); (d) A. Karton and J. M. Martin, J. Chem. Phys. **125**, 144313 (2006); (e) X. Li and J. Paldus, Chem. Phys. Lett. **431**, 179 (2006); (f) X. Li, J. R. Gour, J. Paldus, and P. Piecuch, Chem. Phys. Lett. **461**, 321 (2008).
15. A. I. Boldyrev and J. Simons, J. Phys. Chem. **97**, 6149 (1993).
16. R. Linguerri, N. Komiha, R. Oswald, A. Mitrushchenkov, and P. Rosmus, Chem. Phys. **346**, 1 (2008).
17. I. Magoulas and A. Kalemos, J. Chem. Phys. **139**, 154309 (2013).
18. (a) G. S. Kocheril, H. W. Gao, D. F. Yuan, L. S. Wang, J. Chem. Phys. **157**, 171101 (2022); b) G. S. Kocheril, H. W. Gao, L. S. Wang, Mol. Phys. e2182610 (2023); c) G. S. Kocheril, H. W. Gao, L. S. Wang, J. Chem. Phys. **158**, 236101 (2023); d) H. W. Gao, J. Hui and L. S. Wang, Chem. Commun. **59**, 12431 (2023); e) H. W. Gao, H. W. Choi, J. Hui and L. S. Wang, J. Phys. Chem. A **128**, 3579 (2024).
19. I. León, Z. Yang, H. T. Liu, and L. S. Wang, Rev. Sci. Instrum. **85**, 083106 (2014).
20. B. Dick, Phys. Chem. Chem. Phys. **21**, 19499 (2019).
21. J. Cooper and R. N. Zare, J. Chem. Phys. **48**, 942 (1968).
22. A. Sanov and R. Mabbs, Int. Rev. Phys. Chem. **27**, 53 (2008).
23. I. Leon, Z. Yang, and L. S. Wang, J. Chem. Phys. **138**, 184304 (2013).
24. H. Lefebvre-Brion and R. W. Field. *The Spectra and Dynamics of Diatomic Molecules*. Elsevier, Boston, 2004.
25. C. J. Ballhausen and H. B. Gray. *Molecular Orbital Theory*. Benjamin, New York, 1965.
26. P. Pyykko, Chem. Rev. **88**, 563 (1988).